Icarus 271 (2016) 265–268

Contents lists available at ScienceDirect

Icarus

journal homepage: www.elsevier.com/locate/icarus

The spectrum of Jupiter's Great Red Spot: The case for ammonium hydrosulfide (NH_4SH)

Mark J. Loeffler[a,*], Reggie L. Hudson[a], Nancy J. Chanover[b], Amy A. Simon[a]

[a] NASA Goddard Space Flight Center, Greenbelt, MD 20771, USA
[b] New Mexico State University, Department of Astronomy, Las Cruces, NM 88003, USA

ARTICLE INFO

Article history:
Received 16 December 2015
Revised 2 February 2016
Accepted 3 February 2016
Available online 10 February 2016

Keywords:
Jupiter atmosphere
Ices, UV spectroscopy
Geophysics
Atmospheres, chemistry
Experimental techniques

ABSTRACT

Here we present new ultraviolet–visible spectra of irradiated ammonium hydrosulfide (NH_4SH), a reported jovian atmospheric cloud component, for a range of temperatures and radiation doses and make assignments to the spectral features. We show that the combination of radiolysis and thermal annealing of NH_4SH causes the originally featureless ultraviolet–visible reflectance spectrum to evolve into one that absorbs in the ultraviolet–visible region. Furthermore, we find that our laboratory spectra resemble HST spectra below 500 nm, suggesting that the more stable reaction products of NH_4SH radiolysis are likely an important component of the Great Red Spot.

Published by Elsevier Inc.

1. Introduction

Jupiter's Great Red Spot (GRS) is arguably one of the more recognizable features in the Solar System. The GRS was observed in the nineteenth century and perhaps earlier (Falorni, 1987), and since its discovery many candidate materials have been proposed to explain its color (West et al., 1986). However, no consensus has emerged concerning a unique chromophore, chromophores, or composition. One reason for the difficulty in understanding the GRS's color is that this feature's spectrum lacks distinct absorption bands, possessing only a strong slope below 600 nm and into the ultraviolet region, which results in the aforementioned red appearance (Simon et al. 2015a). We note that the colors associated with the GRS are not as pronounced as is indicated in Voyager and Pioneer images and that the GRS is actually more orange than red (Simon et al., 2015a).

The GRS is believed to originate in jovian tropospheric clouds made of NH_3, NH_4SH, and H_2O (Weidenschilling and Lewis, 1973; Wong et al., 2015). Although a simple explanation for the GRS's color might involve one of these three cloud components in solid form, none of the laboratory reflectance spectra of the corresponding ices is an adequate match at ultraviolet and visible wavelengths (Lebofsky and Fegley, 1976). However, because these same cloud components are exposed to cosmic rays (Whitten et al., 2008) and possibly solar UV photons, they will undergo chemical reactions. Such chemical alterations could contribute to an explanation of jovian colors, but the pursuit of this possibility has been hindered by a lack of laboratory data. Only the photochemical alteration of the ultraviolet–visible (UV–vis) reflectance of NH_4SH has been reported in the refereed literature (Lebofsky and Fegley, 1976), and only at a single temperature far below that of the GRS, and the resulting spectrum does not match that of the GRS.

Given that there is only one published photochemical study of NH_4SH available (Lebofsky and Fegley, 1976) and no radiation-chemical studies, and that there are many variables that could alter the reflectance spectrum of this solid, we investigated whether ion-irradiated ammonium hydrosulfide (NH_4SH) could be an important contributor to the GRS's spectrum. As a radiation source we used ~1 MeV protons (p+), which serve as an analog to low-energy cosmic rays and high-energy cosmic rays that have been slowed down in Jupiter's atmosphere. Our proton-irradiation results also give insight into what changes other energy sources, such as vacuum-UV photons, electrical discharges, and high-energy electrons, might cause as the reaction products and spectral changes induced by various types of energetic processing are often similar (Baratta et al. 2002; Hudson & Moore 2001), although this has not been checked for NH_4SH until now. Our previous work on NH_4SH relied on infrared (IR) spectroscopy to identify radiation products, which were found to be predominantly polysulfur ions and radicals (Loeffler et al., 2015). We now report the first correlations between our infrared studies and the ultraviolet–visible region.

We point out that equilibrium thermodynamic models (Wong et al., 2015) predict that the jovian NH_4SH cloud component is

* Corresponding author. Tel.: +1 301 286 7502.
E-mail address: mark.loeffler@nasa.gov (M.J. Loeffler).

http://dx.doi.org/10.1016/j.icarus.2016.02.010
0019-1035/Published by Elsevier Inc.

stable at higher temperatures than those used in our experiments, the difference being due to a greater pressure in Jupiter's atmosphere than in our sample chamber. Thus, in this study we investigated whether heating our irradiated samples to the predicted NH_4SH cloud temperatures (~200 K; Wong et al. 2015) caused their UV–vis reflectance spectra and color to change significantly and to match GRS observations. Our new laboratory results are presented here, compared with HST spectra of the GRS, and discussed in light of 40 years of research into sulfur chemistry since the early work of Lebofsky and Fegley (1976).

2. Methods

2.1. Laboratory details

The experimental approach and preparation of NH_4SH are described in Loeffler et al. (2015), so only a few points require additional comments. Samples approximately 17 μm thick were irradiated with 0.924 MeV p+ to a fluence of 5×10^{13} ions cm^{-2} (or an average absorbed dose of 2.83 MGy), corresponding to 150 years on Jupiter based on the cosmic-ray energy flux of 9×10^{-3} ergs cm^{-2} s^{-1} (Sagan and Thompson, 1984). The film thickness was chosen to be smaller than the range of the impinging ions (Ziegler, 2010). After irradiation, samples were warmed at 0.4 K min^{-1} to the desired temperature. Before and after various irradiation and warming steps, spectra of NH_4SH were recorded with an Avantes ULS2048XL fiber-optic spectrometer from 250 to 1000 nm at a resolution of 1.5 nm. To make our spectra as comparable as possible to those derived from HST observations, we measured the diffuse reflectance of our ices on a nearly Lambertian aluminum substrate, created by sandblasting the substrate's surface. The incident light was aimed normal (perpendicular) to the sample's surface and the reflected light was collected at an angle of 9° from normal. Again, this small phase angle was chosen to make our results more directly comparable to those from ground-based and HST observations, which are limited in jovian phase angle coverage. The laboratory reflectance spectra shown here were obtained by dividing the intensity (I) of the light collected from the sample by a reference spectrum of the blank substrate, after subtracting a dark-current spectrum from each. This procedure gave the ice's reflectance as $R = (I_{sample} - I_{dark})/(I_{reference} - I_{dark})$. In addition to measuring spectral reflectance, we also photographed our samples with a Canon Eos Rebel T3i camera.

To assess the stability of our equipment, we performed a variety of blank experiments that tested to what degree factors such as source fluctuation, detector drift, and background contamination caused changes to the UV–vis reflectance of our samples. Over the timescale of our experiments, we found that all such reflectance variations due only to our equipment were under 1% over the wavelengths used (250–1000 nm). In addition to the errors determined from these blank experiments, which are errors analogous to the error bars given for the HST data (see below), the various steps in the synthesis, irradiation, and annealing of our NH_4SH ices raised the possibility of sample-to-sample variations. Thus, to assess the reproducibility of our laboratory samples and their spectra, multiple experiments were repeated under identical conditions. Comparisons of the results showed that reflectance values in the initial NH_4SH spectrum in Fig. 1 were reproducible to within 5%, while those of the spectra of irradiated and of irradiated and heated NH_4SH were reproduced to better than 10%.

2.2. HST details

The HST data used in this study were taken from WFPC2 and WFC3 over 20 years (1995–2015). The acquired HST images were converted into absolute calibrated I/F units (reflectance), as described previously (Simon-Miller & Gierasch 2010), so that the spectral characteristics of the GRS could be studied. The data shown here were acquired in pixels covering the central core of the GRS, which is typically the region with the most intense color (Simon et al. 2015a).

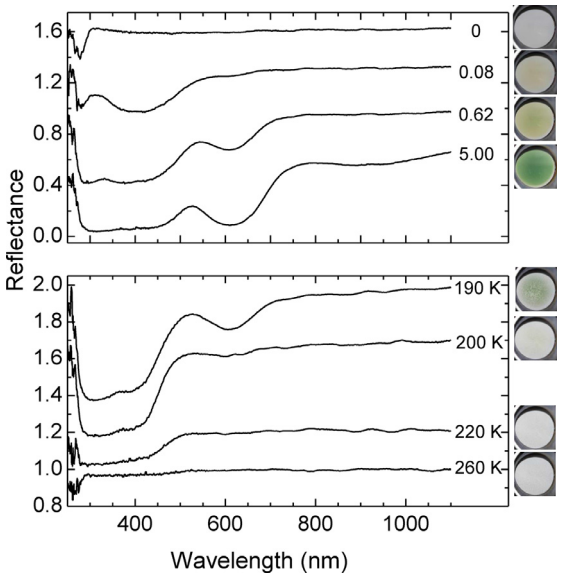

Fig. 1. Ultraviolet–visible reflectance spectra and photographs of initially-crystalline NH_4SH before and after irradiation at 120 K with 0.9 MeV protons, followed by post-irradiation heating. The proton fluence (top panel; units of 10^{13} p+ cm^{-2}) and sample temperature during heating (bottom) are given to the right of the spectra. For clarity, spectra after doses labeled 0, 0.08, and 0.62 have been vertically offset by 0.9, 0.6, and 0.25, while spectra taken at temperatures of 190 K, 200 K, and 220 K have been vertically offset by 1.2, 0.8, and 0.25.

The photometric stability of WFPC2 and WFC3 over time has been monitored using standard stars (Gonzaga et al. 2006, Kalirai et al. 2009, Kalirai et al. 2010). For WFPC2, the UV filters (<336 nm) showed the greatest long-term change with the reflectance of Jupiter varying less than 2–8%, while the longer wavelength filters were stable to within ~2% (see Simon-Miller & Gierasch 2010). The WFC3 photometric performance has been even more stable than WFPC2 2015 with variation of less than 1% (Kalirai et al. 2009, 2010). Possible variations due to the solar flux across the HST pass bands has previously been calculated using data from Colina et al. (1996) and found to be constant within 0.1% over time (Krivova et al. 2009).

3. Results

Fig. 1 shows photographs and the corresponding UV–vis spectra of an initially-crystalline NH_4SH sample before and after proton irradiations at 120 K and during post-irradiation warming. The only absorption in the spectrum of the unirradiated sample is a drop in reflectance below 300 nm, likely from SH^- (Ellis and Golding, 1959; Guenther et al., 2001). On irradiation of the NH_4SH ice, a broad feature appeared near 400 nm, followed by one near 610 nm, and then a much weaker feature near 900 nm. The photographs in the figure show that the irradiated sample had a greenish appearance, a color that was rapidly lost on warming. By about 200 K, the strong green color and the peak near 610 nm were gone, but a spectral slope remained at 300–500 nm that was absent from the initial spectrum. Heating to higher temperatures caused this slope to decrease, yet a weak slope was still observed at 260 K. By room temperature, no slope or absorption remained in the spectrum, indicating that any residual material present did not absorb

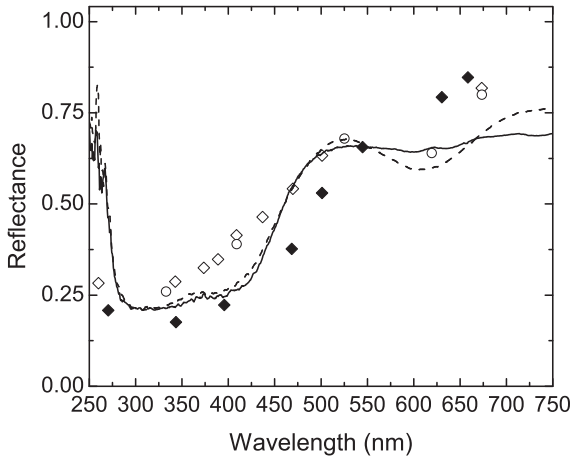

Fig. 2. Comparison of the ultraviolet–visible spectra of irradiated crystalline NH_4SH with HST observations of the GRS from 1995 (o), 2008 (◇), and 2015 (♦). The laboratory spectra are after the sample was irradiated at 120 K and then warmed to 190 K (dashed line) and then 200 K (solid line). The laboratory spectra are vertically offset to match the GRS observational data. Error bars given for the HST data have been described in the text; the error in the 2015 HST data is shown but is smaller than the symbol.

in the wavelength region of Fig. 1. Samples of NH_4SH irradiated at higher temperatures (e.g., 160 K) showed these same trends in color and spectra, suggesting that the spectrum of the sample irradiated at low temperature and warmed to 200 K is representative of the spectrum that would have been produced if irradiation could have been performed at 200 K.

Fig. 2 shows spectral data of the GRS taken over 20 years with the Hubble Space Telescope (Simon et al., 2015a; Simon et al., 2015b), along with our laboratory spectra of irradiated NH_4SH at 190 and 200 K. The 2015 HST data show a significantly different spectrum than in the other years, as the reflectance below 500 nm is lower. This relative darkening may have resulted during the GRS's decreased interaction with the surrounding clouds observed in 2014 (Simon et al., 2014). These clouds often add fresh whiter cloud material to the GRS interior, making for an interesting comparison between the two epochs. Below 500 nm, all the GRS spectra show a strong slope, which begins to decrease in the UV. Above 500 nm, there is more variation in the HST data, as the two latest sets show a relatively weak slope, while the 1995 data shows a drop in reflectance near 620 nm. Determining whether these differences above 500 nm are solely due to NH_4SH is difficult, as CH_4 also absorbs in this region, though with a much narrower absorption feature (Karkoschka and Tomasko, 2010).

4. Discussion

4.1. Spectral assignments and colors

The UV–vis spectra after proton irradiation shown in Fig. 1 are generally consistent with the early photochemical studies on NH_4SH reported by Lebofsky and Fegley (1976). While the radiation-chemical products in NH_4SH are difficult to determine from this spectral region alone, our earlier work (Loeffler et al., 2015) suggested a few spectral assignments. Infrared spectra recorded in our previous studies showed the formation of $S_3^{-\bullet}$, NS_x^-, and S_x^{2-}/HS_x^- in proton-irradiated NH_4SH. The trisulfur anion radical $S_3^{-\bullet}$ has a strong absorbance near 600 nm (e.g., Chivers and Drummond, 1973), therefore we assign the feature seen near that wavelength in Fig. 1 to $S_3^{-\bullet}$. Beyond that, our irradiated samples had a broad absorption at 300–500 nm that agrees with expectations for many polysulfur species, including NS_x^-, and S_x^{2-}/HS_x. An absorption peak has also been reported for S_6^{2-} at positions from 410 to 480 nm in solution (Prestel and Schindewolf, 1987; Dubois et al., 1988; Dubois et al., 1989). Therefore, this ion probably contributes to the absorbance we see increasing near 450 nm after an incident radiation dose of about 1×10^{13} p+ cm^{-2}, since this dose is needed to form sufficient $S_3^{-\bullet}$ monomer radicals for their dimerization to S_6^{2-}. Other contributors to the absorption features seen in Fig. 1 probably include S_2^{2-} (Giggenbach, 1972) and neutral amorphous sulfur (Dubois et al., 1988).

The thermal behavior of our irradiated samples supports our spectral assignments. The only identified radical, $S_3^{-\bullet}$, is the first product to decrease during warming, and it reached the noise level by 200 K, consistent with our previous IR studies (Loeffler et al., 2015). The absorption bands between 300–500 nm, indicative of the other more stable polysulfur species, persist to higher temperatures than does the $S_3^{-\bullet}$ and remain relatively unchanged until above 200 K (Fig. 1), where thermal sublimation becomes increasingly important.

The colors in the photographs of Fig. 1 also support our spectral assignments. The $S_3^{-\bullet}$ radical that we associate with the 600-nm band produces a blue color (Chivers and Elder, 2013), so a second species is needed to form the striking green of irradiated NH_4SH. As the reaction sequence to form the $S_3^{-\bullet}$ radical probably is

$$HS^- \rightarrow S_2^{-\bullet} \rightarrow S_3^{-\bullet} \quad (1)$$

$S_2^{-\bullet}$ is a likely candidate. Its yellow color ($\lambda_{max} \approx 390$ nm), which we observe at lower fluences (see Fig. 1 (top)) coupled with the blue of $S_3^{-\bullet}$, would produce the green shown in Fig. 1. Another likely yellow contributor is the dimer of $S_3^{-\bullet}$, namely S_6^{2-} ($\lambda_{max} \approx 405$ nm). See Chivers and Drummond (1973) and Raulin et al. (2011) for more on $S_2^{-\bullet}$ and S_6^{2-}. Warming the irradiated NH_4SH sample initiated reactions involving free radicals and reactive ions, depleting or removing them before the entire sample, including the larger aforementioned poly-sulfur species, began to sublimate.

4.2. Comparison to remote sensing

As noted previously (e.g., Simon et al. 2015a), the variation in the HST data from 1995 to 2015 comes from the fact that the GRS environment is dynamic. However, even though the GRS spectra appear to change with time in all of the data sets shown, there is always a steep slope at 300–500 nm and a subsequent flattening in the ultraviolet. Our laboratory spectra of irradiated NH_4SH, heated to temperatures associated with the Jovian clouds, provide a reasonable match to this spectral region with the most recent 2015 HST data fitting the best. Above 500 nm, the HST spectra show more variation and thus are more difficult to interpret. Regardless, our laboratory spectrum taken at 190 K reproduces the apparent drop in reflectance observed in the 1995 data, yet as stated earlier it is unclear whether this decrease is solely due to NH_4SH, as this is near a CH_4 gas absorption feature and no finer spectral coverage is available. The laboratory spectrum taken at 200 K is a better fit to the other two HST data sets, which do not show this drop in reflectance at 600 nm, although the HST spectral slope appears to be somewhat steeper. We note that it is this steep slope above 500 nm that causes the visual color difference between our samples and the GRS, which appears orange in the HST images (Simon et al. 2015b).

4.3. Implications for Jupiter's Great Red Spot

Our studies suggest that a cloud layer containing fresh NH_4SH can be modified by cosmic rays, producing a broad absorption at 300–500 nm (e.g., Fig. 1) that is similar to the HST data presented here. Warming our irradiated NH_4SH ices to ~200 K, where

a pristine cloud is expected to be thermally stable (Wong et al., 2015), caused their spectral reflectance to change significantly above 500 nm, with the loss of the $S_3^{-\bullet}$ radical's absorption, to more closely resemble the HST data. The observation that the sample is not more orange in color, as expected from the HST images (Simon et al., 2015b), is a consequence of our sample having a weaker slope above 500 nm, which suggests that another component may be needed to fit the entire spectral range shown. This other component may also be responsible for the slope variation at 300–500 nm in the HST data.

Besides showing that irradiation and warming of NH_4SH produces spectra similar to those of the GRS, it is also important to consider whether the doses used in our studies will accumulate in a NH_4SH cloud at 1–2 bars. Using a rough estimate for the Jovian cosmic-ray energy flux (Sagan and Thompson, 1984), we find that a dose of $\sim 10^{13}$ ions cm^{-2} in our experiments corresponds to about 30 years of cosmic ray exposure, and can produce the broad absorption at 300–500 nm that resembles the HST data. However, considering that the GRS extends to higher altitudes than other cloud features (Simon-Miller et al., 2002) and that NH_4SH has been attributed to the ubiquitous 3 μm absorption observed near the highest altitudes in Jupiter's atmosphere (Sromovsky and Fry, 2010), it seems likely that other, less penetrating, forms of radiation will also be able to modify the NH_4SH grains, shortening this exposure time considerably. Comparing this time to that in which a NH_4SH grain in the GRS is exposed to cosmic rays is desirable, yet measurements are lacking. Instead, we point out that models predict that the material arising in the center of Jupiter's Oval BA should thoroughly mix throughout the entire vortex on a timescale that varies between months (de Pater et al., 2010) and decades (Conrath et al., 1981) depending on the vertical temperature gradient assumed, suggesting that the doses in our experiments are reasonable. It is worth noting that the grain exposure time could be much shorter, as NH_3 grains in Jupiter's atmosphere were only detectable for ~40 h after they first appeared (Reuter et al., 2007). Although in that case it was suggested that another material might be coating grains (Atreya et al., 2005; Reuter et al., 2007), no such thin coating could impede cosmic ray ions from altering the underlying grain material.

Given the resemblance between our laboratory spectra and HST data below 500 nm and the theoretical predictions that NH_4SH is an important cloud component in Jupiter's troposphere it seems possible that the reaction products of NH_4SH radiolysis contribute to the spectrum of the GRS, and possibly to other colored regions of Jupiter. To better quantify the results reported here, future work is also needed along the lines of, for example, measurements of the optical constants of the unirradiated and irradiated NH_4SH ice, which would enable a full radiative-transfer analysis of the NH_4SH cloud component. Laboratory measurements of NH_4SH in the near-IR region used by observers would also be useful, as there may be additional absorption bands diagnostic of NH_4SH and its radiolysis products. In addition, experiments in which NH_4SH is doped with trace amounts of impurities, such as hydrocarbons, that are believed to be present in the jovian atmosphere might also prove useful, particularly in determining whether their addition could improve spectral fits at longer wavelengths.

Acknowledgments

The support of NASA's Planetary Atmospheres and Outer Planets Research programs is gratefully acknowledged. Steve Brown, Tom Ward, and Eugene Gerashchenko, members of the NASA Goddard Radiation Effects Facility, operated and maintained the Van de Graaff accelerator. This work used NASA/ESA Hubble Space Telescope observations retrieved from the Data Archive at the Space Telescope Science Institute, which is operated by the Association of Universities for Research in Astronomy, Inc. under NASA contract NAS 5-26555. The observations are associated with programs GO5313, GO11498, and GO13937, and using these program numbers all data can be retrieved from http://archive.stsci.edu/hst/search.php at the Hubble archive.

References

Atreya, S.K., Wong, A.S., Baines, K.H., et al., 2005. Jupiter's ammonia clouds—localized or ubiquitous? Planet. Space Sci. 53, 498–507.
Chivers, T., Drummond, I., 1973. The chemistry of homonuclear sulphur species. Chem. Soc. Rev. 2, 233–248.
Chivers, T., Elder, P.J.W., 2013. Ubiquitous trisulfur radical anion: Fundamental and applications in materials science, electrochemistry, analytical chemistry, and geochemistry. Chem. Soc. Rev. 42, 5996–6005.
Colina, L., Bohlin, R.C., Castelli, F., 1996. The 0.12 – 0.25 μm absolute flux distribution of the Sun for comparison with solar analog stars. Astron. J. 112, 307–315.
Conrath, B.J., Flasar, F.M., Pirraglia, J.A., et al., 1981. Thermal structure and dynamics of the Jovian atmosphere. II - Visible cloud features. J. Geophys. Res. 86, 8769–8775.
de Pater, I., et al., 2010. Persistent rings in and around Jupiter's anticyclones – Observations and theory. Icarus 210, 742–762.
Dubois, P., Lelieur, J.P., Lepoutre, G., 1988. Chemical-species in sulfur ammonia solutions - Influence of amide addition. Inorg. Chem. 27, 3032–3038.
Dubois, P., Lelieur, J.P., Lepoutre, G., 1989. Photochemical observations in solutions of sulfur in liquid ammonia. Inorg. Chem. 28 pp. 2489–2391.
Ellis, A.J., Golding, R.M., 1959. Spectrophotometric determination of the acid dissociation constants of hydrogen sulfide. J. Chem. Soc. Faraday Trans. I 127–130.
Falorni, M., 1987. The discovery of the Great Red Spot of Jupiter. J. Brit. Astron. Assoc. 97, 215–219.
Giggenbach, W., 1972. Optical-spectra and equilibrium distribution of polysulfide ions in aqueous-solution at 20°. Inorg. Chem 11, 1201–1207.
Gonzaga, S., Brammer, G., Heyer, I., et al., 2006. WFPC2 Standard Star Monitoring Memo. STScI Tech. Rep.
Guenther, E.A., Johnson, K.S., Coale, K.H., 2001. Direct ultraviolet spectrophotometric determination of total sulfide and iodide in natural waters. Anal. Chem 73, 3481–3487.
Kalirai, J.S., MacKenty, J., Rajan, A., et al., 2009. The Photometric Performance and Calibration of WFC3/UVIS. STScI Instrument Science Report WFC3 2009–2031.
Kalirai, J.S., Baggett, S., Borders, T., et al., 2010. The Photometric Performance of WFC3/UVIS: Temporal Stability Through Year 1. STScI Instrument Science Report WFC3 2010–2014.
Karkoschka, E., Tomasko, M.G., 2010. Methane absorption coefficients for the jovian planets from laboratory, Huygens, and HST data. Icarus 205, 674–694.
Krivova, N.A., Solanki, S.K., Wenzler, T., et al., 2009. Reconstruction of solar UV irradiance since 1974. J. Geophys. Res. 114, 7 pp.
Lebofsky, L.A., Fegley, M.B., 1976. Laboratory reflection spectra for determination of chemical composition of icy bodies. Icarus 28, 379–387.
Loeffler, M.J., Hudson, R.L., Chanover, N.J., et al., 2015. Giant-planet chemistry: Ammonium hydrosulfide (NH_4SH), its IR spectra and thermal and radiolytic stabilities. Icarus 258, 181–191.
Prestel, H., Schindewolf, U., 1987. Identification of the main sulfur nitrogen-compounds in sulfur ammonia solutions. Z. Anorg. Allg. Chem 551, 21–32.
Raulin, K., Gobeltz, N., Vexin, H., et al., 2011. Identification of the EPR signal of S_2^- in green ultramarine pigments. Phys. Chem. Chem. Phys. 13, 9253–9259.
Reuter, D.C., et al., 2007. Jupiter cloud composition, stratification, convection, and wave motion: A view from new horizons. Science 318, 223–225.
Sagan, C., Thompson, W.R., 1984. Production and condensation of organic gases in the atmosphere of titan. Icarus 59, 133–161.
Simon-Miller, A.A., et al., 2002. New observational results concerning Jupiter's Great Red Spot. Icarus 158, 249–266.
Simon, A.A., et al., 2015a. Spectral comparison and stability of red regions on Jupiter. J. Geophys. Res. Planets 120, 483–494.
Simon, A.A., Wong, M.H., Orton, G.S., 2015b. First results from the Hubble OPAL program: Jupiter in 2015. Astrophys. J. 82, 8.
Simon, A.A., et al., 2014. Dramatic Change in Jupiter's Great Red Spot from spacecraft observations. Astrophys. J. L797.
Simon-Miller, A.A., Gierasch, P.J., 2010. On the Long-Term Variability of Jupiter's Winds and Brightness as Observed from Hubble. Icarus 210, 258–269.
Sromovsky, L.A., Fry, P.M., 2010. The source of 3-μm absorption in Jupiter's clouds: Reanalysis of ISO observations using new NH_3 absorption models. Icarus 210, 211–229.
Weidenschilling, S.J., Lewis, J.S., 1973. Atmospheric and cloud structures of Jovian planets. Icarus 20, 465–476.
West, R.A., Strobel, D.F., Tomasko, M.G., 1986. Clouds, aerosols, and photochemistry in the Jovian atmosphere. Icarus 65, 161–217.
Whitten, R.C., Borucki, W.J., O'Brien, K., et al., 2008. Predictions of the electrical conductivity and charging of the cloud particles in Jupiter's atmosphere. J. Geophys. Res. 113. doi:10.1029/2007JE002975, 7 pages.
Wong, M.H., Atreya, S.K., Kuhn, W.R., et al., 2015. Fresh clouds: A parameterized updraft method for calculating cloud densities in one-dimensional models. Icarus 245, 273–281.
Ziegler, J. F., 2010. Stopping and range of ions in matter SRIM2010 (available at www.srim.org).